Targeted Deletion of *fgl2* Leads to Impaired Regulatory T Cell Activity and Development of Autoimmune Glomerulonephritis[1]

Itay Shalev,[2]* Hao Liu,[2]* Cheryl Koscik,* Agata Bartczak,* Mojib Javadi,* Kit Man Wong,* Asif Maknojia,* Wei He,* Ming Feng Liu,* Jun Diao,* Erin Winter,* Justin Manuel,* Doug McCarthy,† Mark Cattral,*‡ Jennifer Gommerman,† David A. Clark,* M. James Phillips,* Reginald R. Gorczynski,*†‡ Li Zhang,*†§ Greg Downey,*¶ David Grant,*‡ Myron I. Cybulsky,*§ and Gary Levy[3]*†¶

Mice with targeted deletion of fibrinogen-like protein 2 (*fgl2*) spontaneously developed autoimmune glomerulonephritis with increasing age, as did wild-type recipients reconstituted with $fgl2^{-/-}$ bone marrow. These data implicate FGL2 as an important immunoregulatory molecule and led us to identify the underlying mechanisms. Deficiency of FGL2, produced by $CD4^+CD25^+$ regulatory T cells (Treg), resulted in increased T cell proliferation to lectins and alloantigens, Th 1 polarization, and increased numbers of Ab-producing B cells following immunization with T-independent Ags. Dendritic cells were more abundant in $fgl2^{-/-}$ mice and had increased expression of CD80 and MHCII following LPS stimulation. Treg cells were also more abundant in $fgl2^{-/-}$ mice, but their suppressive activity was significantly impaired. Ab to FGL2 completely inhibited Treg cell activity in vitro. FGL2 inhibited dendritic cell maturation and induced apoptosis of B cells through binding to the low-affinity FcγRIIB receptor. Collectively, these data suggest that FGL2 contributes to Treg cell activity and inhibits the development of autoimmune disease. ***The Journal of Immunology,*** **2008, 180: 249–260.**

The FGL2/fibroleukin is a member of the fibrinogen-related protein superfamily of proteins (1, 2). FGL2 was first cloned from human CTLs, and its protein structure deduced from the nucleotide sequence showed a high degree of homology to fibrinogen β and γ subunits (3). FGL2 has been shown to play an important role in innate immunity as an immune coagulant expressed by activated reticuloendothelial cells (macrophages and endothelial cells) (4–6) and has been implicated in the pathogenesis of several inflammatory disorders, including viral hepatitis (7–10), allo- and xenograft rejection (11–13), and cytokine induced fetal loss (14, 15). In a previous report (13), we showed that Ab to FGL2 ameliorated allograft rejection. Furthermore, cardiac grafts from $fgl2^{-/-}$ mice were resistance to thrombosis, suggesting a role for endothelial cell *fgl2* expression in the fibrin deposition associated with allo- and xenotransplantation rejection. In contrast, Ning et al. (13) and Hancock et al. (16) showed that $fgl2^{-/-}$ mice rejected fully mismatched allografts, supporting the contention that the endothelium, but not leukocytes, maybe more important for fibrin deposition in allotransplant rejection.

In addition, Marazzi and Ruegg (17, 18) reported that both $CD4^+$ and $CD8^+$ T cells spontaneously secrete FGL2 with preferential expression in $CD45R0^+$ memory T cells. They suggested that secreted FGL2, which is devoid of prothrombinase activity, might have immune regulatory activity (17). Our lab provided the first evidence that FGL2 also plays a role in acquired immune responses by demonstrating its immunosuppressive activity on dendritic cells (DC)[4] and T cells (19). In vitro, recombinant FGL2 inhibited T cell proliferation in response to anti-CD3/CD28 Abs, Con A, and alloantigens. Moreover, FGL2 promoted a Th2 cytokine profile in allogeneic cultures and inhibited DC maturation by preventing NF-κB nuclear translocation (19).

Recently, Rudensky, Herman, and Kronenberg (20–26) have reported increased expression of *fgl2* in regulatory T cells including $CD4^+CD25^+Foxp3^+$ regulatory T cells (Treg) and $CD8\alpha\alpha^+$ T cells, and proposed that *fgl2* is a putative Treg effector gene. In this study, we showed that Treg cell function was completely inhibited by Ab to FGL2. We further demonstrated that suppressive activity of Treg cells from $fgl2^{-/-}$ mice was impaired, resulting in increased DC, T, and B cell immune reactivity and development of autoimmune renal disease. Collectively, these data support the notion that FGL2 contributes to Treg cell function and has important immunoregulatory activity.

Materials and Methods

Mice

$fgl2^{-/-}$ and $fgl2^{+/+}$ mice were previously generated and the methodology for their production has previously been described (7). In brief, $fgl2^{-/-}$

*Multi Organ Transplant Program, †Department of Immunology, ‡Department of Surgery, §Department of Laboratory Medicine and Pathology, and ¶Department of Medicine, University of Toronto, Toronto, Ontario, Canada

Received for publication May 15, 2007. Accepted for publication October 16, 2007.

The costs of publication of this article were defrayed in part by the payment of page charges. This article must therefore be hereby marked *advertisement* in accordance with 18 U.S.C. Section 1734 solely to indicate this fact.

[1] This work was supported in part by grants from the Heart and Stroke Foundation of Canada (T5686) and the Canadian Institutes for Health Research (GR13298, 79561, and STP 53882).

[2] I.S. and H.L. contributed equally to this study.

[3] Address correspondence and reprint requests to Dr. Gary Levy, Toronto General Hospital, 585 University Avenue, Toronto, Ontario M5G 2C2, Canada. E-mail address: glfgl2@attglobal.net

[4] Abbreviations used in this paper: DC, dendritic cell; Treg, regulatory T cell; PAS, periodic acid-Schiff; BM, bone marrow; MLR, mixed lymphocyte reaction; PI, propidium iodide; PALS, peri-arteriolar lymphoid sheath; GC, germinal center.

Copyright © 2007 by The American Association of Immunologists, Inc. 0022-1767/07/$2.00

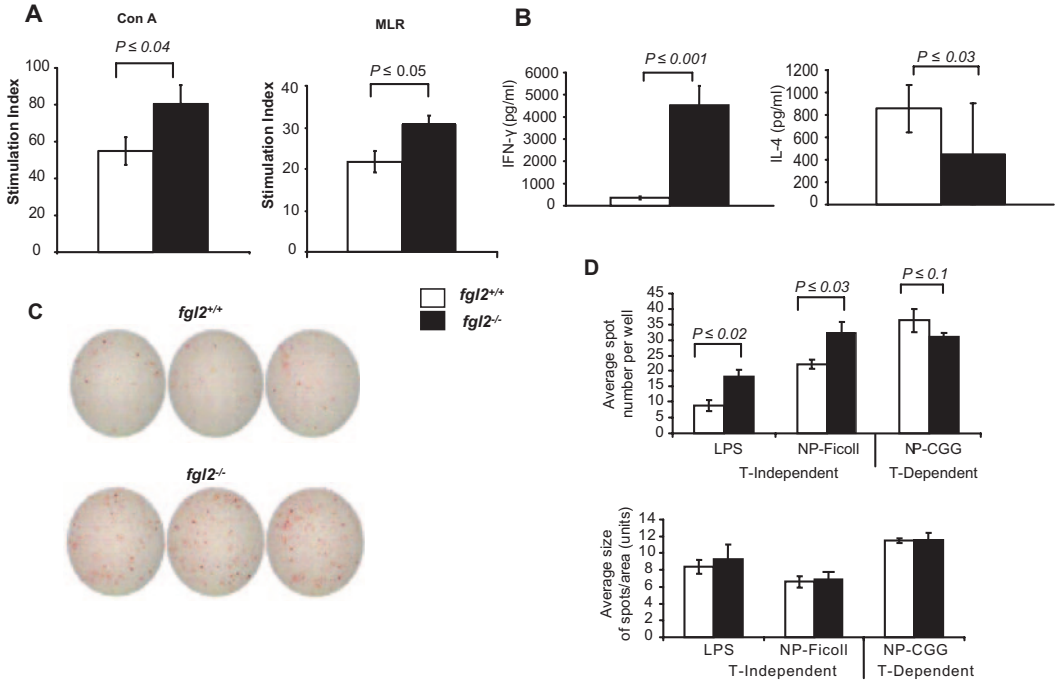

FIGURE 1. Increased reactivity of B and T cells from $fgl2^{-/-}$ mice. *A*, T cell proliferation in response to Con A stimulation and in a MLR as measured by [^{3}H]thymidine (1μCi) incorporation; $n = 6$. *B*, Levels of IFN-γ (*left*) and IL-4 (*right*) in supernatants from MLR reactions, taken at 24 h poststimulation as assessed by sandwich ELISA; $n = 3$. *C* and *D*, Mice were injected with LPS, NP-Ficoll, or NP-CGG. At 5–12 days after injection, spleens were isolated and subjected to ELISPOT analysis. Representative pictures of triplicate ELISPOT wells from $fgl2^{+/+}$ and $fgl2^{-/-}$ mice stimulated with LPS are shown. The number of spots per well (*top right*) is representative of the number of B cells producing Ab per well. Average spot size (*bottom right*) is a measure of the amount of Ab being produced per B cell; $n = 3$. Graphs in all panels show mean ± SEM.

mice were generated by transfecting 129Sv embryonic stem cells with the knockout construct (also derived from 129Sv). These stem cells were then injected into C57BL/6 blastocysts and the resultant chimeras were backcrossed for 10 generations onto a C57BL/6 background (7). $fgl2^{+/+}$ mice were used as controls. BALB/c and $Fc\gamma RIIB^{-/-}$ mice were obtained from The Jackson Laboratory. Mice were housed in the animal facility at Princess Margaret Hospital and treated under the guidelines provided by the University Health Network. Male and female mice used for assays were 6 to 8 wk old unless specified in the text.

Tissue mass and quantification

Mice were anesthetized with pentobarbital. Blood was collected by cardiac puncture, and serum samples were stored at −80°C. Tissues were dissected and fat and connective tissue were removed. Before weighing, tissues were rinsed with PBS to remove blood and excess fluid was removed.

Tissue fixation and sectioning

Frozen tissue was prepared by embedding in OCT (Fisher)-filled cryomolds (TissueTek) and snap frozen in liquid nitrogen. For paraffin-embedded preparations, dissected tissues were immersed in 10% formalin and fixed for 24 h, which were then embedded in paraffin and sectioned in the Pathology Department at the Hospital for Sick Children. Paraffin sections, five microns thick, were stained using standard H&E and periodic acid-Schiff (PAS) staining protocols (7).

Renal function

Serum creatinine was analyzed in the Department of Biochemistry, Univeristy Health Network using an Ektachem 700 analyzer as previously described (7). Urine was collected from mice and analyzed for pH, presence of protein, blood, glucose, and ketones by Labstix purchased from Bayer HealthCare.

Histopathology and immunohistochemistry

Kidneys were obtained and histological sections were stained with PAS or H&E (27). Glomerular and vascular deposition of IgG, IgM, and IgA was determined by staining frozen sections with rat anti-IgG, anti-IgA, and IgM mAb, followed by alkaline phosphatase labeled goat anti-rat Ig conjugates as previously described (27). C3 deposits were examined by direct staining with alkaline phosphatase labeled goat anti-mouse C3 (Cappel Laboratories).

Treg cell isolation

For real-time PCR gene studies, $CD4^+CD25^+$ Treg cells and $CD4^+CD25^-$ T cells were purified with an EasySep Mouse $CD4^+$ T Cell Enrichment Kit (StemCell Technologies) according to manufacturer's instructions followed by FACS using a FACSAria cell sorter (BD Biosciences). Purity of cell populations was ≥98%. For other experiments, $CD4^+CD25^+$ Treg cells and $CD4^+CD25^-$ T cells were purified using a FACSAria cell sorter with purity of ≥90–95%.

Splenocyte isolation

Spleens were dissected, flushed with PBS using a syringe and needle, and cut up into small pieces (<0.5 cm), which were passed through a nylon filter to separate cells from connective tissue. Mononuclear cells were separated from erythrocytes using a Lympholyte M (Cedarlane Laboratories). To release DC, spleens were digested with collagenase D (Roche Diagnostics) for 45 min at 37°C, cell suspensions were then separated using Lympholyte M.

DC generation from bone marrow (BM) precursors and stimulation with LPS

BM was isolated and cultured as previously described (19). In brief, BM was flushed from tibia and femurs, and erythrocytes and T cells were subsequently removed using Lympholyte M and MAC (Miltenyi Biotec), respectively. The remaining BM fractions were cultured on plastic petri dishes (Nunc) for 2 h to remove adherent macrophages. BM was cultured for 7 days in RPMI 1640 medium supplemented with 10% FBS, 800U/ml GM-CSF, and 500U/ml IL-4 (Sigma-Aldrich). After 7 days, cultures were stimulated with 1 μg/ml O5:B55 LPS (Sigma-Aldrich).

T cell proliferation assay

Splenocytes were cultured for 3 days in α-MEM supplemented with 10% FBS, after which 1μCurie [^{3}H]thymidine (Amersham Biosciences) was added to each well. Eighteen hours later, cells were harvested using the

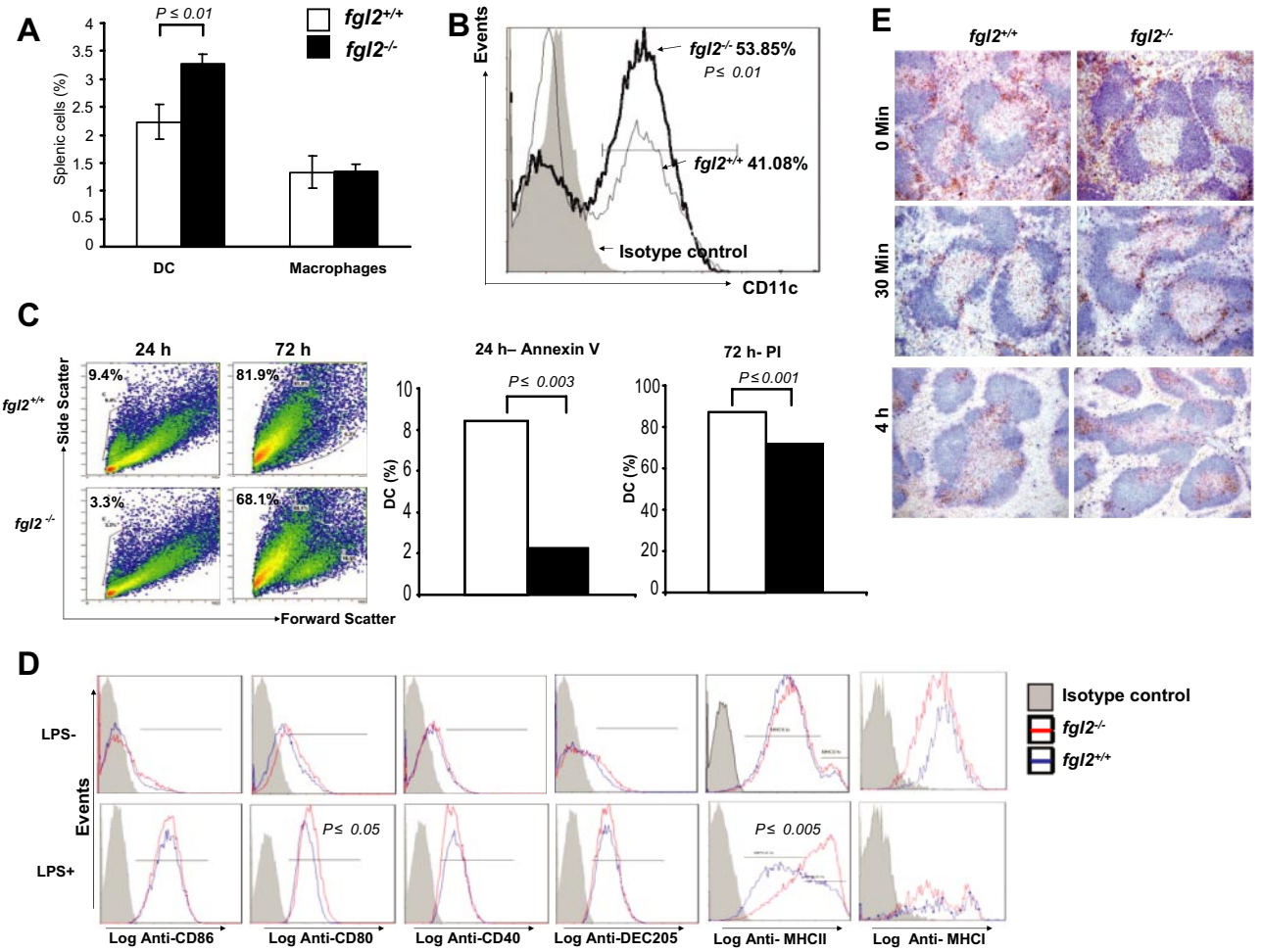

FIGURE 2. Increased numbers and reactivity of DC from *fgl2*$^{-/-}$ mice. *A*, The percentage of DC (CD11c^{+}MHCII^{+}) and macrophages (CD11b^{+}MHCII^{+}) in spleen of *fgl2*$^{+/+}$ and *fgl2*$^{-/-}$ mice. Graph shows mean ± SEM; $n = 6$. *B*, Representative flow cytometry plot of BM-derived DC stimulated with 1 μg/ml LPS; $n = 6$. *C*, BM-derived DC from *fgl2*$^{+/+}$ and *fgl2*$^{-/-}$ mice were harvested at 24 h and 72 h after LPS stimulation and stained with PI and Annexin V. Live and dead cells were first differentiated on the basis of forward and side scatter (*left*). Numbers beside outlined areas indicate a representative percentage of dead cells in the designated gate. Representative flow cytometry values of Annexin V^{+} DC at 24 h (*left*) and PI^{+} DC at 72 h (*right*) are shown. *D*, Expression of surface molecules on DC with and without LPS stimulation by flow cytometry. BM-derived DC were cultured with 800 U/ml GM-CSF and 500U/ml IL-4 for 7 days. A total of 1 μg/ml LPS was then added and cells were cultured for another 18 h to induce maturation and induction of high levels of costimulatory molecules. Control cultures did not receive LPS and therefore represent the expression profile of immature DC. *E*, Kinetics of DC movement in the spleens of *fgl2*$^{+/+}$ and *fgl2*$^{-/-}$ mice. Mice were i.v. injected with 1.5 μg/g of body weight LPS and sacrificed at times 0, 30 min, 1, 2, and 4 h after receiving LPS. Frozen sections were subsequently stained with CD11c (brown) and B220 (blue). Movement from the bridging junction into the PALS is complete between 2 and 4 h. Sections at 1 h and 2 h are similar to sections at 30 min and 4 h, respectively (our unpublished data).

UNIFILTER-96 Filtermate Harvester (PerkinElmer) and counted by Packard Microplate Scintillation Counter.

One-way mixed lymphocyte reaction (MLR)

fgl2$^{-/-}$ or *fgl2*$^{+/+}$ responder splenocytes (4×10^5/100 μl) were stimulated with irradiated BALB/c splenic mononuclear cells (4×10^5/100 μl). Stimulator BALB/c splenocytes were irradiated with 30 Gy using Nordin Gamma Irradiator to prevent cell division.

Con A stimulation

Splenocytes were plated at a concentration of 2×10^5 cells/well in 200 μl of medium and stimulated with 5 μg/ml Con A (Sigma-Aldrich).

Abs used for flow cytometry

Detection Abs included: FITC-B220, PE-B220, FITC-CD11b, FITC-CD11c, PE-CD11c, PE-Cy5-CD11c, FITC-CD3, PE-Cy5-CD3, FITC-CD4, PE-Cy7-CD25, PE-Foxp3, PE-CD40, FITC-CD8α, PE-CD8α, PE-CD80, PE-CD86, PE-IgD, FITC-IgM, and PE-Cy5-NK1.1. Isotype controls included: FITC-armenian hamster IgG, FITC-mouse IgG2a, PE-mouse IgG2a, PE-mouse IgG2b, FITC-rat IgG2a, PE-rat IgG2a, PE-Cy5-rat IgG2a, PE-rat IgG2b, and PE-Cy5-rat IgG2b. All Abs were obtained from Cedarlane Laboratories, BD Pharmingen, or eBioscience.

Cell labeling and analysis

Cell suspensions were washed and suspended in PBS containing 3.5% mouse serum (Cedarlane Laboratories) at a final concentration of 1×10^7cells/ml to block Fc receptors. A total of 100 μl of the cell suspension was aliquoted into 5 ml polypropylene test tubes, and Ab was added and incubated for 30 min at 4°C. Ab binding was assessed using a Coulter Epics-XL-MCL flow cytometer and data were analyzed using CXP/RXP software (Beckman Coulter). Live cells were gated according to forward and side scatter parameters.

Annexin V and propidium iodide (PI) labeling

A total of 100 μl of cell suspension (containing 1×10^6 cells), 10 μl of Annexin-V (SouthernBiotech) was added and incubated at 4°C for 15 min. A total of 380 μl of binding buffer was added along with PI (SouthernBiotech) and incubated for another 15 min before analysis by flow cytometry.

ELISA

Supernatants were removed from MLR cultures at 24- and 48-h time points. Cytokine profiles were obtained using IL-4, IL-2, and IFN-γ ELISA kits (Pierce). ELISA was performed according to the kit instructions. Plates were coated with anti-cytokine Ab; supernatant samples were incubated on the plates for 2 h at 37°C. Cytokine binding was detected by using a secondary HRP-conjugated anti-cytokine Ab. Tetramethylbenzidine substrate was used as a chromogenic substrate. Absorbance was measured at 450 nm.

ELISPOT

B cells were purified from spleens of mice using the MACS purification system. Purified B cells (1×10^3/well) were incubated on Millipore plates coated with anti-IgM and detected with a biotin-conjugated secondary Ab. Spots were developed using the AEC substrate set (BD Biosciences) and detected with ELISPOT Reader series 3A Analyzer. Ab production was induced by injection of LPS, NP-Ficoll, or NP-CGG.

Immunization protocol

Mice were i.v. injected with LPS (Sigma-Aldrich) at a dose of 1.5 μg/g of body weight. NP-Ficoll (Sigma-Aldrich) and NP-CGG (Biosearch Technologies) were given by intraperitoneal injection at 30 μg and 100 μg doses, respectively. Mice were euthanized 5 days after LPS injection and 12 days following treatment with NP-Ficoll or NP-CGG. Alum precipitation of NP-CGG was performed to prepare the reagent for injection. First, 400 μl of aluminum potassium sulfate (Sigma-Aldrich) per 100 μg NP-CGG were combined. Protein was precipitated by the addition of 1N potassium hydroxide and the precipitate was then washed three times with PBS and 100 μg NP-CGG with alum was injected intraperitoneally (28).

Generation of BM chimeras

Reciprocal transplants were performed between *fgl2*$^{+/+}$ and *fgl2*$^{-/-}$ donors and recipients. Donor BM cells were prepared as previously described for the generation of in vitro DC cultures. Two days before irradiation and 2 wk after transplantation, mice were given clavamox in their drinking water to prevent infection. Recipients were irradiated with 11 Gy using a Nordon Gamma Irradiator and immediately i.v. injected with 5×10^6 BM cells. Two months after injection, chimeric mice were euthanized and cells were harvested and analyzed.

Real-time PCR

Following the purification of splenic CD4$^+$CD25$^+$ and CD4$^+$CD25$^-$ T cells by FACS, RNA was extracted from the cells and the levels of *fgl2* mRNA expression were measured by real-time PCR. *fgl2* expression levels were normalized to HPRT, GAPDH and RPL13, which served as housekeeping genes. The $2^{-\Delta CT}$ calculations were used to present levels of *fgl2* expression in CD4$^+$CD25$^+$ relative to CD4$^+$CD25$^-$ T cells.

Suppression assay

In vitro suppression assays used cultures of 2×10^4 CD4$^+$CD25$^-$ T cells from *fgl2*$^{+/+}$ mice as responder cells, together with 8×10^4 irradiated splenocytes as APC and titrated numbers of CD4$^+$CD25$^+$ Treg cells from either *fgl2*$^{-/-}$ or *fgl2*$^{+/+}$ mice as suppressor cells. Cultures were stimulated with Con A (1 μg/ml) for 72 h and [^{3}H]thymidine was added for the last 18 h to measure proliferation of effector T cells. For Ab blockade studies, titrated concentrations of a mAb to FGL2 (no. H00010875-M01 monoclonal IgG2a Ab; Abnova) were added to the cell cultures of CD4$^+$ effector T cells and CD4$^+$CD25$^+$ Treg cells sorted from wild-type mice, at a 1:4 suppressor:responder cell ratio in the presence of APC and Con A.

FGL2 effects on APCs

The effect of FGL2 on the LPS-induced maturation of BM-derived DC was examined by adding recombinant FGL2 to DC cultures during LPS-induced maturation (19). BM cells from C57BL/6 and *FcγRIIB*$^{-/-}$ mice were prepared and cultured for 7 days in the presence of GM-CSF and IL-4 to derive immature DC. Immature DC were stimulated with LPS (200 ng/ml) to reach final maturation for 2 days in the presence of fibrinogen (negative control) or FGL2 (10 μg/ml). The expression of surface maturation markers, including CD80, CD86, and MHCII molecules, were measured with specific Abs and isotype controls by flow cytometric analysis.

The A20 B cell line was obtained from American Type Culture Collection and the A20IIA1.6 mutated B cell line was a gift from Dr. James Booth (Sunnybrook Research Institute, Toronto, ON). The cells were stained with anti-FcγRIIB/III Ab (2.4G2; BD Pharmingen) and biotinylated FGL2 (2 μg) as previously described (29). A total of 2×10^5 A20 and A20IIA1.6 cells were cultured with RPMI 1640 medium containing 10% FBS in 48 well tissue culture plates (Corning). Cells treated with 500 nM staurosporine, 500 nM FGL2, or 500 nM fibrinogen (negative control) for 12 h, were stained with either PI or FAM-VAD-FMK (poly caspases activation marker) and analyzed by flow cytometry for cell apoptosis.

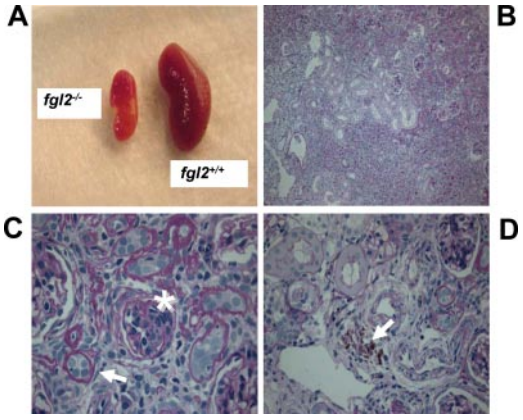

FIGURE 3. Kidney defect observed in 7- to 12-mo-old *fgl2*$^{-/-}$ mice. *A*, Gross appearance of a *fgl2*$^{-/-}$ kidney that developed a severe glomerulonephritis compared with the littermate control. *B–D*, Histology of the defective kidney from *fgl2*$^{-/-}$ mice stained with PAS. *B*, Intense cellular infiltration and fibrin deposition (10× magnification). *C*, Mesangial expansion of the glomerulus (asterisk) and collapsed tubules surrounded by fibrin (arrow) (40× magnification). *D*, Brown staining (arrow) is hemosiderin staining of macrophages and indicates the presence of hemorrhage (40× magnification).

Statistical analysis

Statistical significance was assessed by a Student's *t* test or by ANOVA; differences with $p \leq 0.05$ were considered significant.

Results

Gross morphology, histology, and mass of fgl2$^{-/-}$ *mice*

The generation of *fgl2*$^{-/-}$ has been previously described (7). Gross morphology and histology of tissues and organs from young (6–8 wk) and old (7 mo) *fgl2*$^{-/-}$ and *fgl2*$^{+/+}$ mice were compared. In young *fgl2*$^{-/-}$ mice, all organs appeared normal as assessed by gross appearance, histological analysis, and weight; however, 25% fewer Peyer's Patches were found in the small intestine. Decreased number of intestinal Peyer's Patches and follicles was also found in older *fgl2*$^{-/-}$ mice. Although 6 to 8-wk-old *fgl2*$^{-/-}$ and *fgl2*$^{+/+}$ control mice exhibited similar body weights, at 7 mo of age, *fgl2*$^{-/-}$ mice were significantly smaller in size and weight ($p \leq 0.05$). By 7 mo of age, kidney size and weight were smaller in 25% of *fgl2*$^{-/-}$ mice as compared with *fgl2*$^{+/+}$ mice. Spleens were enlarged in *fgl2*$^{-/-}$ mice compared with littermate controls (data not shown).

Constitutive FGL2 expression

The LacZ reporter gene inserted into exon 1 of the *fgl2*$^{-/-}$ construct was used to examine constitutive FGL2 expression (7). β-galactosidase activity was detected in lymphoid organs, including BM, thymus (our unpublished data), lymph nodes, and spleen. β-galactosidase staining was also detected in the stomach and intestine, which was localized primarily to the lamina propria, consistent with reports by others (17) (data not shown). Presence of FGL2 protein was compared by immunohistochemistry. In particular, heart and intestine stained strongly for presence of FGL2 (data not shown).

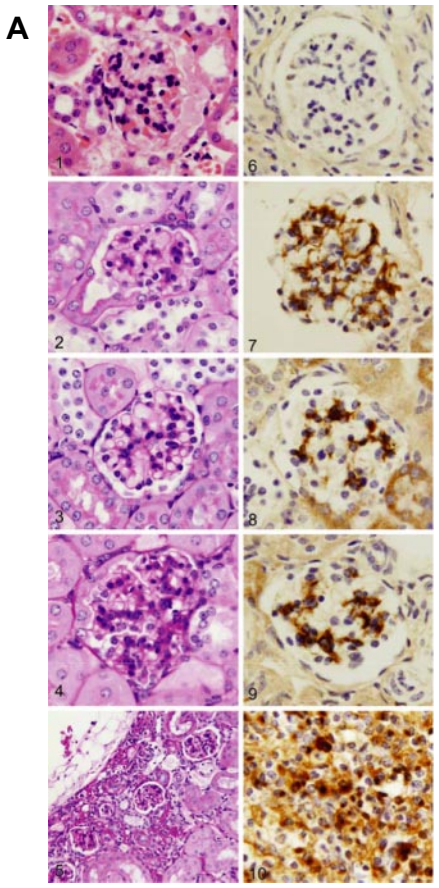

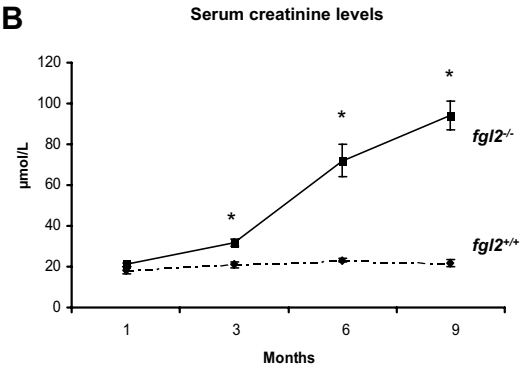

C

Urinalysis of *fgl2*$^{-/-}$ mice

Age (months)	1	2	3	4	5	6	9
Blood	-	+	+	++	++	+++	+++
Ketones	-	-	-	-	-	-	-
Glucose	-	-	-	-	-	-	-
Protein (g/L)	0	0.12±0.07	0.58±0.17	1.8±0.49	9.8±4.16	16.6±3.4	20
pH	-	6	6	6	6	6	6

Urinalysis of *fgl2*$^{-/-}$ mice was performed at different time points. The levels of blood, ketones, glucose, protein and pH are shown. Protein levels are presented as the mean ± SEM. Blood levels are shown as + for mild, ++ for moderate and +++ for high (n=5).

FIGURE 4. The evolution of autoimmune glomerulonephritis. *A-1*, Kidney from wild-type mouse at 6 mo. Normal glomerulus. HE, × 400. *A-2–A-10*, Kidneys from *fgl2*$^{-/-}$ mice. *A-2*, At 1 mo, glomeruli show slight focal mesangial thickening. Tubules are normal. PAS × 400. *A-3*, At 3 mo, glomeruli show slight mesangial thickening and slightly increase in cellularity. Capillary loops widely patent. Tubules are normal. PAS × 400. *A-4*, At 6 mo, glomeruli show prominent mesangial thickening and there is increase in cellularity. Capillary loops hard to visualize. Tubules are normal. PAS × 400. *A-5*, At 6 mo, another area showing marked glomerular changes with global mesangial thickening, sclerosis, and loss of vascularity. Note also loss of tubules, interstitial inflammatory cell infiltrate, sclerosis, and collapse of parenchyma. PAS × 200. *A-6*, At 6 mo, IgG isotype control. Note glomerulus in the center with increased cellularity and surrounding renal parenchyma with inflammatory cell infiltrate and fibrosis. Sever glomerulonephritis. This control immunoperoxidase stain is negative. IP × 400. *A-7*, At 6 mo, immunoperoxidase stain for IgG. The glomerular mesangium is positively stained. IP × 400. *A-8*, At 6 mo, immunoperoxidase stain for IgM. The glomerular mesangium is positively stained. IP × 400. *A-9*, At 6 mo, immunoperoxidase stain for IgA. The glomerular mesangium is positively stained. IP × 400. *A-10*, At 6 mo, immunostaining of cellular infiltrate for IgG. Many of the infiltrating cells are positive. The same result was seen with IgM and IgA (data not shown). IP × 400. *B*, Levels of creatinine in the serum of *fgl2*$^{-/-}$ and *fgl2*$^{+/+}$ mice. Data represent as mean ± SEM; $n = 5$, ∗, $p \leq 0.05$. *C*, Urinalysis of *fgl2*$^{-/-}$ mice. Urinalysis of *fgl2*$^{-/-}$ mice was performed at different time points. The levels of blood, ketones, glucose, protein, and pH are shown. Blood levels are shown as + for mild, ++ for moderate, and +++ for high. Protein levels are presented as mean ± SEM; $n = 5$.

Increased reactivity of B and T cells from fgl2$^{-/-}$ *mice*

Previous studies (19) from our laboratory suggested that FGL2 has immunosuppressive activity. To further explore the effects of FGL2 on the immune system, we examined the proportion and activity of T and B cells from *fgl2*$^{-/-}$ mice. Although we found similar proportions of T cells (CD4$^+$ and CD8$^+$) and B cells (IgM$^+$ and IgD$^+$) in the spleens of *fgl2*$^{-/-}$ and *fgl2*$^{+/+}$ mice. T and B cells from *fgl2*$^{-/-}$ mice were shown to have increased reactivity and effector T cells were polarized toward a Th1 response. T cells from *fgl2*$^{-/-}$ mice had increased proliferation in response to Con A ($p \leq 0.04$) and in a one way MLR ($p \leq 0.05$) (Fig. 1*A*), consistent with our previous in vitro data, which showed that FGL2 inhibited T cell proliferation (19). Th1 and Th2 cytokine profiles were analyzed by ELISA. IFN-γ, a Th1 cytokine, was found to be markedly increased, whereas the production of the Th2 cytokine IL-4 was diminished in supernatants from the MLR cultures of *fgl2*$^{-/-}$ responder cells (Fig. 1*B*).

Type-1 (TI-1), Type-2 (TI-2) T cell-independent, and T cell-dependent (TD) B cell responses were analyzed by ELISPOT. In response to the TI Ags, LPS ($p \leq 0.02$), and NP-Ficoll ($p \leq 0.03$), increased numbers of Ab-producing B cells from *fgl2*$^{-/-}$ mice were seen (Fig. 1, *C–D*). However, the amount of Ab produced per cell as indicated by the size of the spot was similar in B cells from *fgl2*$^{+/+}$ and *fgl2*$^{-/-}$ mice. *fgl2*$^{-/-}$ mice immunized with the T-dependent Ag NP-CGG had similar numbers of Ab-producing B cells and equivalent Ab production per cell as *fgl2*$^{+/+}$ mice. These data indicate that FGL2 is involved in the regulation of T-independent B cell responses, which require help from APCs, but not T-dependent B cell responses.

Increased numbers and reactivity of DC from fgl2$^{-/-}$ *mice*

In the spleen of *fgl2*$^{-/-}$ mice, we observed a 30% increase in the proportion and absolute numbers of DC (CD11c$^+$MHCII$^+$) ($p \leq 0.01$) (Fig. 2*A*), whereas the proportions of macrophages (CD11b$^+$MHCII$^+$) were similar between *fgl2*$^{-/-}$ and *fgl2*$^{+/+}$ mice. A significant increase in the number of DC obtained from in vitro BM cultures was seen in *fgl2*$^{-/-}$-derived DC cultures ($p \leq 0.01$; Fig. 2*B*). We further examined the proportions of DC subsets

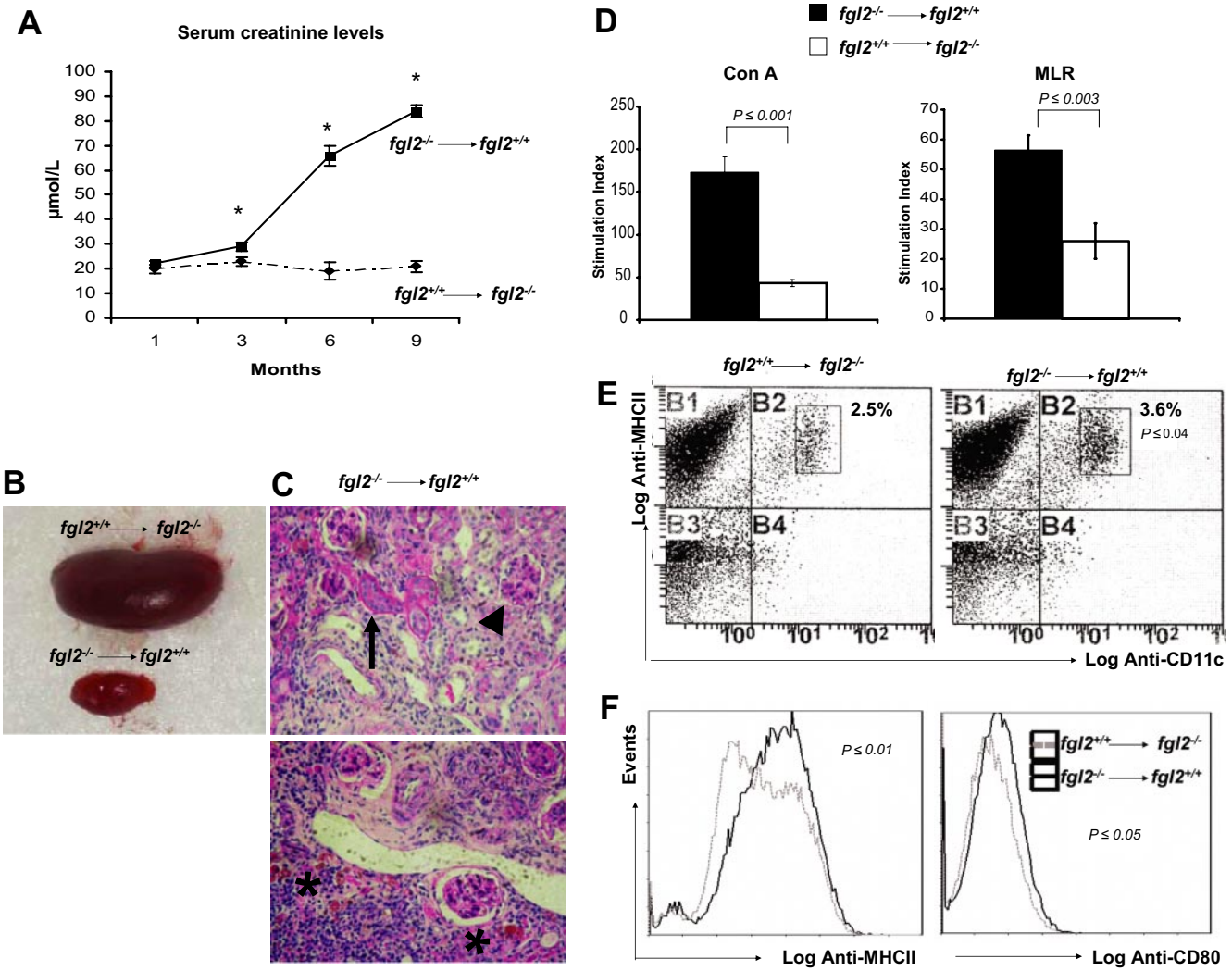

FIGURE 5. $fgl2^{+/+}$ recipients reconstituted with $fgl2^{-/-}$ BM exhibit the phenotype of $fgl2^{-/-}$ mice. $fgl2^{-/-}$ and $fgl2^{+/+}$ mice were irradiated with 11 Gy of γ-irradiation before injection with BM from $fgl2^{+/+}$ and $fgl2^{-/-}$ mice, respectively; assays were preformed following BM reconstitution. *A*, Levels of creatinine in the serum of $fgl2^{-/-}$ and $fgl2^{+/+}$ BM-reconstituted mice at different time points (indicated by number of months) following BM reconstitution. Data represent mean ± SEM; $n = 5$, ∗, $p \leq 0.05$. *B*, Gross appearance of a defective kidney from $fgl2^{-/-}$ BM-reconstituted mice, which developed a severe glomerulonephritis. The kidney was small in size and displayed histological abnormalities. *C*, Evidence of mesangial expansion (arrowhead), collapsed tubules (arrow), cellular infiltrates, fibrin deposition, and hemosiderin staining (asterisks) were shown with PAS staining. *D–F*, Two months following BM reconstitution, splenocytes, and BM were harvested from each treatment group for analysis of the development and function of T cells and DC. *D*, T cell proliferation in response to Con A or in a MLR. Data represent as mean ± SEM. *E*, Flow cytometry of DC ($CD11c^+MHCII^+$) in spleen of $fgl2^{-/-}$ and $fgl2^{+/+}$ BM-reconstituted mice. Numbers indicate a representative percentage of cells in the designated gate. *F*, Representative expression of costimulatory molecules on the surface of BM-derived DC by flow cytometry.

in lymphoid tissues based on the expression of B220, CD11b, and CD8α. In $fgl2^{-/-}$ mice, we observed an increase in all plasmacytoid and myeloid DC subsets rather than an increase in a specific subset (our unpublished data).

The increase in the number of DC present in the spleen and BM of $fgl2^{-/-}$ mice could be explained by an abnormal proliferation of DC precursors or an increase in DC lifespan. Forward and side scatter plots showed that DC derived from $fgl2^{+/+}$ mice at 24 and 72 h post-LPS stimulation contained more dead cells than cultures of DC derived from $fgl2^{-/-}$ mice. Cultures were stained with Annexin V and PI to assess for apoptosis. At 24 h post-LPS stimulation, there was a 3-fold increase in the proportion of DC staining positive for Annexin V in $fgl2^{+/+}$ cultures as compared with cultures of DC from $fgl2^{-/-}$ mice. At 72 h, nearly all DC from $fgl2^{+/+}$ mice stained positive for PI (Fig. 2*C*), whereas in $fgl2^{-/-}$ cultures, a smaller population of DC stained positive. Thus in the absence of *fgl2*, apoptosis of LPS-stimulated DC in culture is both decreased and delayed.

Unstimulated DC generated from BM cultures from both $fgl2^{-/-}$ and $fgl2^{+/+}$ mice expressed similarly low levels of CD80, CD86, CD40, MHCII, MHCI, and DEC205. DC from both $fgl2^{-/-}$ and $fgl2^{+/+}$ mice after LPS stimulation showed increased expression of these maturation markers. However, we observed higher levels of CD80 and MHCII expression in DC from $fgl2^{-/-}$ mice (Fig. 2*D*). These data collectively suggest that DC from $fgl2^{-/-}$ mice are increased in numbers and achieve greater activation following LPS stimulation.

The migration rate of DC from the bridging junction to periarteriolar lymphoid sheath (PALS) of the spleen following LPS stimulation was assayed by immunohistochemistry. Murine DC in the spleen reside in the bridging junctions between the PALS and B cell follicle, and upon antigenic stimulation, migrate into the

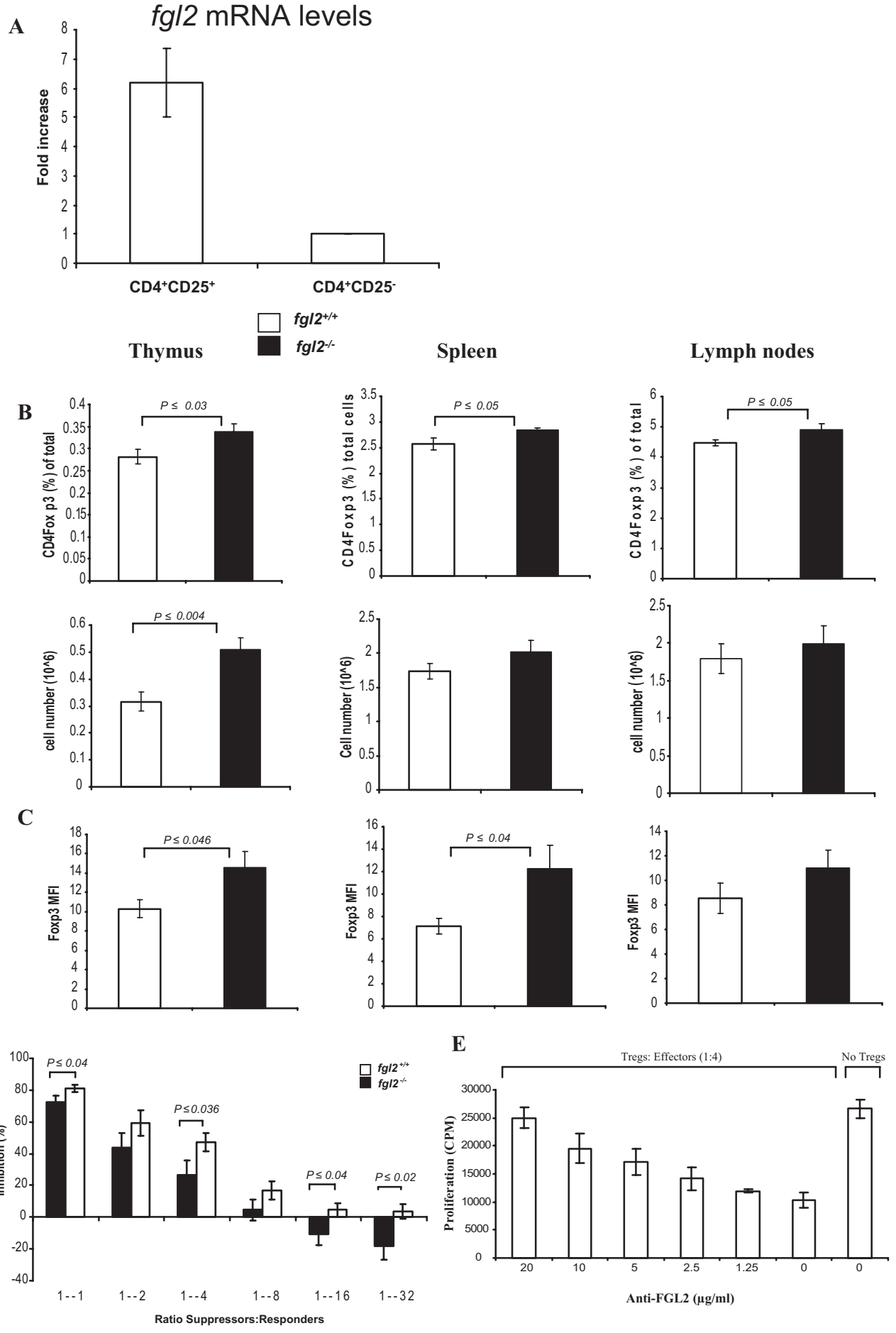
A
fgl2 mRNA levels
Fold increase
CD4+CD25+
CD4+CD25-
fgl2+/+
fgl2-/-
Thymus
Spleen
Lymph nodes
B
CD4Fox p3 (%) of total
P ≤ 0.03
CD4Foxp3 (%) total cells
P ≤ 0.05
CD4Foxp3 (%) of total
P ≤ 0.05
cell number (10^6)
P ≤ 0.004
Cell number (10^6)
cell number (10^6)
C
Foxp3 MFI
P ≤ 0.046
Foxp3 MFI
P ≤ 0.04
Foxp3 MFI
D
Inhibition (%)
P≤ 0.04
P≤0.036
P≤ 0.04
P≤ 0.02
1--1
1--2
1--4
1--8
1--16
1--32
Ratio Suppressors:Responders
E
Tregs: Effectors (1:4)
No Tregs
Proliferation (CPM)
20
10
5
2.5
1.25
0
0
Anti-FGL2 (µg/ml)

PALS. At time 0 (preinjection), splenic DC from both $fgl2^{+/+}$ and $fgl2^{-/-}$ mice were localized to the bridging junctions between the PALS and B cell follicle. By 2–4 h post-LPS injection, DC migrated to the PALS in both $fgl2^{+/+}$ and $fgl2^{-/-}$ mice. However, comparison of DC staining in the PALS at 30 min and 1 h post-LPS stimulation showed that DC in $fgl2^{-/-}$ mice moved into the PALS at a faster rate (Fig. 2*E*), although this was not statistically significant.

Normal spleen architecture and formation of germinal centers (GC) was observed in $fgl2^{-/-}$ *mice*

To assess whether *fgl2* is important for splenic organization and GC formation, $fgl2^{-/-}$ and $fgl2^{+/+}$ mice were injected with saline (control) or NP-CGG (a T cell-dependent Ag). Spleens from each group were harvested at 12 days postimmunization and analyzed by immunohistochemistry and flow cytometry. Distribution of T and B cells was visualized by staining tissue sections with anti-CD3 and anti-B220 Abs. In both $fgl2^{+/+}$ and $fgl2^{-/-}$ spleens, a clear interface between the T cell-rich PALS and surrounding B cell follicles was observed. The MAdCAM-1-stained marginal sinus, which separates the marginal zone from the outer follicular region of the B cell follicle was evident in both $fgl2^{-/-}$ and $fgl2^{+/+}$ spleens. Furthermore, extensive peanut agglutinin staining, the GC B cell marker, was observed in the PALS of both $fgl2^{-/-}$ and $fgl2^{+/+}$ spleens following immunization with NP-CGG. This was confirmed by flow cytometry analysis of GC B cells ($B220^+GL7^+Fas^+$) (data not shown).

Development of autoimmune glomerulonephritis in $fgl2^{-/-}$ *mice*

With age, $fgl2^{-/-}$ mice lost weight and by 6 mo, 25% of $fgl2^{-/-}$ aged mice developed severe glomerulonephritis, with characteristically small and yellow kidneys (Fig. 3*A*). Staining of kidneys with PAS reaction revealed extensive infiltration of mononuclear cells and interstitial fibrosis (Fig. 3*B*). Many renal tubules had collapsed and were surrounded with fibrin, and mesangial expansion was evident in the glomerulus (Fig. 3*C*). Hemosiderin staining of macrophages indicated the presence of hemorrhage within the kidney (Fig. 3*D*). Such kidney defects were not observed in $fgl2^{+/+}$ mice at any age up to 9 mo ($n = 20$).

To further explore the renal abnormality observed in 6- to 12-mo old $fgl2^{-/-}$ mice, kidneys were harvested from $fgl2^{-/-}$ mice at 1, 3, and 6 mo and examined by routine histology and stained for the presence of immunoglobulins (IgA, IgG, and IgM). Histological examination of kidneys at different time points was done on H&E stained sections (Fig. 4*A*). Kidney structure was normal at 1 mo. In particular the glomeruli were normal, aside from very minimal mesangial thickening. By 3 mo there was focal segmental mesangial thickening and mild increase in cellularity of glomeruli (Fig. 4*A*). By 6 mo the glomerular changes were severe and widespread with generalized increase in cellularity, marked mesangial thickening and marked decrease in vascularity. Additionally, at 6 mo there was also a heavy interstitial inflammatory cell infiltration comprised predominantly of lymphocytes. There was also marked tubular loss, interstitial sclerosis, and fibrosis (Fig. 4*A*). Immunoperoxidase staining for IgG, IgM, and IgA was strongly positive in glomeruli and in infiltrating cells (Fig. 4*A*). Kidneys from wild-type mice were normal at all times. C3 deposits were detected in kidneys from $fgl2^{-/-}$ mice at 1, 3, and 6 mo coincident with deposits of immunoglobulins.

Urine and serum analysis were also performed at different time points and revealed progressive increases in the levels of protein (albumin) and blood in the urine (Fig. 4*C*) and increases in serum creatinine (Fig. 4*B*) in $fgl2^{-/-}$ mice with age. In contrast, in wild-type mice the levels of albumin and blood in the urine (our unpublished data) and serum creatinine (Fig. 4*B*) were normal at all times. The levels of IgG and IgM autoantibodies against dsDNA, ssDNA, or chromatin in aged $fgl2^{-/-}$ mice were normal and comparable to aged wild-type mice (our unpublished data).

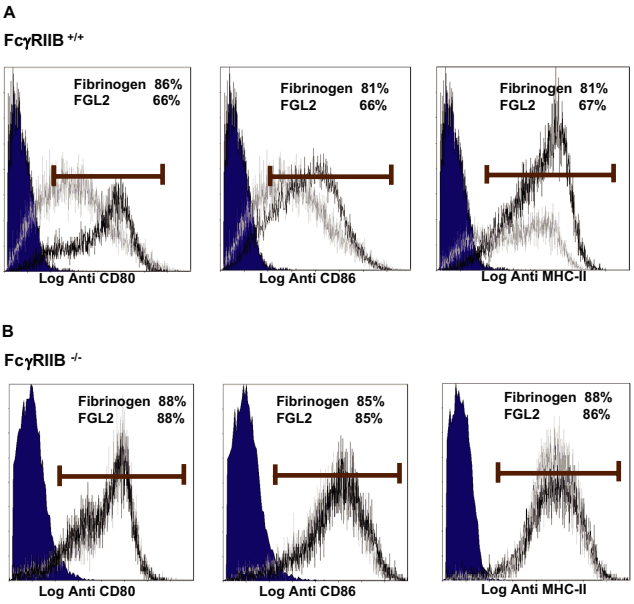

FIGURE 7. FGL2 inhibits the maturation of BM-derived DC through binding to inhibitory FcγRIIB receptor. BM cells from C57BL/6 and $FcγRIIB^{-/-}$ mice were prepared and cultured for 7 days in the presence of GM-CSF and IL-4 to derive immature DC as described in *Materials and Methods*. Immature DC were stimulated with LPS (200 ng/ml) to reach final maturation for 2 days in the presence of fibrinogen (negative control) or FGL2 (10 μg/ml). The expression of surface maturation markers including CD80, CD86, and MHCII were measured by flow cytometry. Gray histograms show fluorescence signals of cells treated with FGL2 and stained with the specific Abs. Black histograms represent cells treated with fibrinogen. The blue shaded areas are the appropriate isotype-matched Ig control. *A*, The expression of CD80, CD86, and MHCII on BM-derived DC from C57BL/6 mice was decreased by FGL2 treatment. *B*, The expression of maturation markers of BM-derived DC from $FcγRIIB^{-/-}$ mice was not affected by FGL2 treatment.

FIGURE 6. FGL2 contributes to Treg cell activity. *A*, Levels of *fgl2* mRNA expression in $CD4^+CD25^+$ relative to $CD4^+CD25^-$ T cells as measured by real-time PCR. *B*, Flow cytometry measurement of $CD4^+Foxp3^+$ Treg cell percentage in spleen, lymph nodes, and thymus (*top*); calculated absolute $CD4^+Foxp3^+$ Treg cell number in lymphoid organs (*bottom*). *C*, Mean fluorescence intensity (MFI) of Foxp3 expression in Treg cells from $fgl2^{-/-}$ and $fgl2^{+/+}$ mice by flow cytometry. *D*, In vitro suppression assays using cultures of $CD4^+CD25^-$ T cells from $fgl2^{+/+}$ mice as responder cells, together with APC and titrated numbers of $CD4^+CD25^+$ Treg cells from either $fgl2^{-/-}$ or $fgl2^{+/+}$ mice as suppressor cells. [^{3}H]Thymidine incorporation was used to measure the proliferation of effector T cells. The activity of Treg cells was expressed as a percent suppression of $CD4^+$ effector T cell proliferation in the absence of Treg cells. *E*, Titrated concentrations of anti-FGL2 Ab were added to the cultures of $CD4^+CD25^-$ T cells and $CD4^+CD25^+$ Treg cells in the presence of APC. All graphs in panel represent mean ± SEM from three independent experiments of two to four mice in each group.

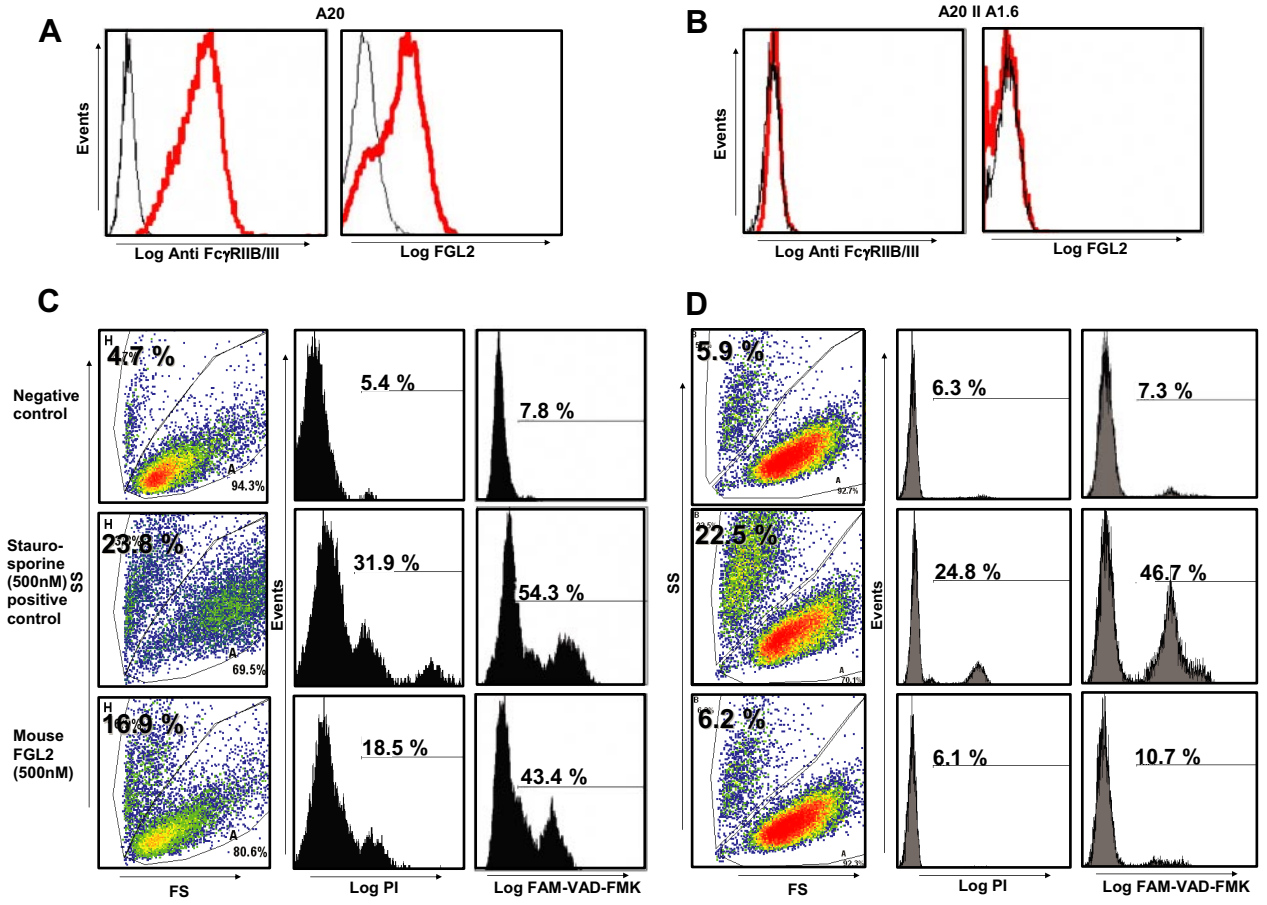

FIGURE 8. FGL2 induces apoptosis in A20 B cells but not in FcγRIIB mutated A20IIA1.6 B cells. *A*, *Left panel*, A20 cells stained with anti-FcγRIIB/III Ab (red histogram) but not with isotype Ab control (black histogram). *Right panel*, biotinylated FGL2 (2 μg) bound to A20 cells (red) and anti-FcγRIIB/III Ab blocked its binding (black). *B*, In A20IIA1.6 cells, there is neither positive staining with anti-FcγRIIB/III Ab (*left panel*) nor positive binding with FGL2 (*right panel*). *C*, Induction of apoptosis in A20 cells. Cells were treated with negative control (*first row*), 500 nM staurosporine (*second row*), or FGL2 (*third row*) for 12 h, stained with either PI or FAM-VAD-FMK (poly caspases activation marker) and analyzed by flow cytometry. Dot plot in the *left panel* displays the forward scatter against side scatter properties. Dead cells with low forward scatter and high side scatter were counted in gate H. PI and FAM-VAD-FMK staining is shown in *middle* and *right panel*, respectively. Both staurosporine and FGL2 showed apoptosis induction effects. *D*, Staurosporine also induced apoptosis in A20IIA1.6 cells but FGL2 failed to induce apoptosis in A20IIA1.6 cells. Results are representative of three experiments.

fgl2$^{+/+}$ *recipients reconstituted with* fgl2$^{-/-}$ *BM exhibit the phenotype of* fgl2$^{-/-}$ *mice*

We generated BM chimeras to determine whether the etiology of the increased immune reactivity of *fgl2*$^{-/-}$ mice was hemopoietic. Mice were sublethally irradiated and *fgl2*$^{+/+}$ mice were reconstituted with *fgl2*$^{-/-}$ BM, whereas *fgl2*$^{-/-}$ mice were reconstituted with *fgl2*$^{+/+}$ BM. Populations of macrophages, T cells, B cells, and DC purified from each of the transplant groups by MACS were genotyped to confirm that reconstitution had occurred (our unpublished data). By three months after BM reconstitution, elevated levels of creatinine were measured in the serum of *fgl2*$^{+/+}$ mice reconstituted with *fgl2*$^{-/-}$ BM (Fig. 5*A*), and one of these mice developed a severe kidney defect as seen in *fgl2*$^{-/-}$ aged mice. The kidney was small in size (Fig. 5*B*) and displayed the following histological features: intense cellular infiltrate, fibrin deposition, expanded mesangial matrix of some glomeruli, and collapsed tubules. Hemosiderin staining was also present indicating hemorrhage (Fig. 5*C*). Mice were followed for up to 9 mo and similar kidney abnormalities were seen in all *fgl2*$^{+/+}$ mice reconstituted with *fgl2*$^{-/-}$ BM.

In addition, *fgl2*$^{-/-}$ BM-reconstituted mice exhibited increased proliferation of T cells in response to alloantigens and Con A (Fig. 5*D*), increased numbers of DC (Fig. 5*E*) with increased expression of cell surface CD80 and MHCII compared with *fgl2*$^{+/+}$ BM-reconstituted mice (Fig. 5*F*).

FGL2 contributes to Treg cell activity

Previous studies (21–26) have reported increased expression of *fgl2* mRNA transcripts in Treg cells and suggested a role for *fgl2* as a putative Treg cell effector gene. To examine this possibility, we first assessed the expression of *fgl2* in Treg cells. CD4$^+$CD25$^+$ T cells and CD4$^+$CD25$^-$ T cells were purified from spleens of C57BL/6 mice by FACS and *fgl2* transcript levels were measured by real-time PCR. A 6-fold increase of *fgl2* mRNA in CD4$^+$CD25$^+$ T cells compared with CD4$^+$CD25$^-$ T cells was seen (Fig. 6*A*).

To determine whether *fgl2* was important for the generation and maintenance of Treg cells, we analyzed the proportion of Treg cells in the lymphoid tissues of *fgl2*$^{+/+}$ and *fgl2*$^{-/-}$ mice. Following isolation, mononuclear cells isolated from various lymphoid tissues were stained with mAbs against CD4, CD3, Foxp3, and CD25 and analyzed by flow cytometry. A statistically significant increase in the percentage of Treg cells was observed in all lymphoid tissues of *fgl2*$^{-/-}$ mice compared with littermate controls (Fig. 6*B*). This increase corresponded to a higher absolute number of Treg cells in all lymphoid organs (Fig. 6*B*). Foxp3

expression levels were increased in Treg cells from $fgl2^{-/-}$ mice compared with littermate controls (Fig. 6*C*).

We directly assessed the effect of targeted deletion of *fgl2* on the ability of Treg cells to suppress effector $CD4^+$ T cell proliferation. Purified $CD4^+CD25^-$ T cells from $fgl2^{+/+}$ mice were cultured for 4 days in the presence of irradiated splenocytes, which served as a source of APC, Con A (1 μg/ml), and in the presence of titrated numbers of $CD4^+CD25^+$ T cells purified from either $fgl2^{-/-}$ or $fgl2^{+/+}$ mice. [^{3}H]Thymidine incorporation was used to measure the proliferation of effector $CD4^+$ T cells. Treg cells from $fgl2^{-/-}$ mice were less efficient in suppressing $CD4^+$ T cell proliferation compared with Treg cells from $fgl2^{+/+}$ mice at all ratios used (Fig. 6*D*). Surprisingly, at ratios 1:16 and 1:32 of Treg cells to effector T cells, we observed stimulation and proliferation of $CD4^+$ T cells in cultures to which Treg cells from $fgl2^{-/-}$ mice had been added. One possible explanation could be a contamination of effector T cells from $fgl2^{-/-}$ mice, which were previously shown to have a hyperproliferative response to Con A and alloantigens. In a separate set of experiments, we examined the ability of anti-FGL2 mAb to block Treg cell activity. Titrated concentrations of anti-FGL2 Ab were added to cultures of effector T cells and Treg cells at a 1:4 suppressor:responder cell ratio in the presence of APC. Anti-FGL2 Ab completely blocked the suppressive activity of Treg cells in a dose dependent manner (Fig. 6*E*). In contrast, an isotype control Ab had no inhibitory effect.

FGL2 mediates its activity through binding to inhibitory FcγRIIB receptor expressed by APC

Previously, we reported that recombinant FGL2 generated in CHO cells binds to DC and B cells through binding to inhibitory FcγRIIB receptor (29). To examine the biological significance of the binding of FGL2 to the receptor, BM DC were isolated from wild-type and $Fc\gamma RIIB^{-/-}$ mice (C57BL/6 background), and cultured in the presence of GM-CSF and IL-4 for 7 days. Immature DC were stimulated for 48 h with LPS (200 ng/ml) in the presence of fibrinogen (negative control) or FGL2 (10 μg/ml). Treatment with FGL2 resulted in reduced expression of CD80, CD86, and MHCII expression in DC from wild-type mice (Fig. 7*A*), whereas FGL2 treatment had no inhibitory effect on DC from $Fc\gamma RIIB^{-/-}$ mice (Fig. 7*B*).

To study the effect of FGL2 on B cells, the A20 B cell line was cultured for 12 h in the presence of FGL2 (500 nM) or fibrinogen used as a negative control. Recombinant FGL2 bound to A20 cells, which express FcγRIIB (Fig. 8*A*), resulting in apoptosis. A20 cells treated with FGL2 contained 43.4% positive cells for FAM-VAD-FMK (poly caspases activation marker), indicative of cells undergoing apoptosis, and 18.5% PI positive cells, indicative of dead cells (Fig. 8*C*). In contrast, no apoptosis was observed in cells incubated in the presence of fibrinogen (Fig. 8*C*). A20IIA1.6 cells, which do not express FcγRIIB, did not bind FGL2 and did not undergo apoptosis (Fig. 8, *B* and *D*). Staurosporine (500 nM) was used as a positive control to induce apoptosis in both A20 and A20IIA1.6 cell lines. These results suggest that FGL2 exerts its immunoregulatory effects through the inhibitory FcγRIIB receptor expressed by DC and B cells.

Discussion

FGL2 consists of 432 aa and contains a C-terminal fibrinogen-related domain, which is a highly conserved region found in the β- and γ-chains of fibrinogen and is characteristic of proteins within the fibrinogen superfamily (1, 2). Members of this functionally diverse superfamily include the extracellular matrix proteins tenascin, angiopoietin, growth factors, and ficolin (19). These proteins have been shown to exhibit coagulant and angiogenic activity, as well as immunoregulatory activity (1, 2, 30). Similar to other members of the fibrinogen superfamily, our laboratory has recently discovered (19) that FGL2 inhibits murine DC maturation and adaptive T cell immune responses, in addition to its role in innate immunity through its ability to activate the coagulation system (7–15).

In this present study, we examined the effects of targeted deletion of *fgl2* on the immune system and its role as a negative regulator in vivo. As we had hypothesized, *fgl2* deficiency resulted in increased immune reactivity. We first observed increased numbers of DC in the spleen and BM-derived cultures from $fgl2^{-/-}$ mice following LPS stimulation. This was accompanied by an enhanced expression of maturation markers including CD80 and MHCII, as well as an increased life span of DC from $fgl2^{-/-}$ mice. The increased numbers and activation of DC seen in the $fgl2^{-/-}$ mice were consistent with the inhibitory effect of FGL2 on DC in vitro, which we have previously reported (19). T cells from $fgl2^{-/-}$ mice showed greater proliferation in response to Con A and alloantigens. High levels of IFN-γ, a Th1 cytokine, and low levels of IL-4, a Th2 cytokine, were detected in allogeneic cultures of $fgl2^{-/-}$ responder T cells, demonstrating polarization toward a Th1 immune response. Again, these findings are consistent with in vitro data, showing the ability of FGL2 to inhibit T cell proliferation and promote a Th2 cytokine profile (19). Also, as one might have predicted based on previous studies, we found that DC from $fgl2^{-/-}$ mice had increased CD80 expression but no change in the expression of CD86 (19).

Hancock et al. (16) also examined the effects of targeted deletion of *fgl2* on immune responses, in particular Th1 activity. They reported that Th1 responses and T cell proliferation in response to bacterial and viral infections were comparable in $fgl2^{-/-}$ and $fgl2^{+/+}$ mice. In addition, they showed that the proportions of B cells, macrophages, and $CD4^+$ and $CD8^+$ T cell populations were similar. This is consistent with our findings that equivalent proportions of B cells, T cells, and macrophages are found in the spleens of $fgl2^{-/-}$ and $fgl2^{+/+}$ mice. Our group and Hancock et al. are in agreement with the fact that the Th1 response in $fgl2^{-/-}$ mice is not diminished or impaired. Our group has, in fact, reported an increase in the Th1 immune response. The transplant data in both studies (13, 16) were also similar with comparable rejection rates in $fgl2^{-/-}$ and wild-type recipient mice. Again, our group has also extended these findings to report an increased survival of grafts from $fgl2^{-/-}$ mice (13), an issue which was not examined by Hancock et al. (16). Although some differences seen in the phenotype of our $fgl2^{-/-}$ mice compared with mice reported by Hancock et al. (16) could be attributed to the different methodologies used to generate the two sets of mice (7, 16), we suggest that differences in experimental design are equally plausible as an explanation. For example, Hancock et al. (16) used a potent immunogen to examine immune responses and reported a high IFN-γ level in serum (40 ng/ml); in contrast, we have used a lesser stimulus in vitro which generated only 4 ng/ml IFN-γ (Fig. 1*B*). Hancock et al. (16) suggested that FGL2 might contribute to pathologically significant coagulative responses under certain conditions, just as we have shown in response to MHV-3 but not to endotoxin (7). Hancock et al. (16) and we have raised the possibility that FGL2 plays important roles in responses, which have yet to be fully evaluated, and our data are not in disagreement with this prediction.

With age, our $fgl2^{-/-}$ mice lost weight compared with littermate controls and developed glomerulonephritis and renal failure as indicated by histology and by increased levels of serum creatinine and protein and blood in the urine. The first evidence to suggest that the renal disease may be autoimmune was the marked

infiltration of mononuclear cells in the kidneys and deposits of IgG, IgM, IgA, and complements (C3) in association with renal disease. Secondly, the disease was recapitulated in BM chimera studies. We examined the effect of aging on both numbers and function of Treg cells in *fgl2*$^{-/-}$ mice. One-year-old *fgl2*$^{-/-}$ mice had significantly reduced numbers of Treg cells and their function was impaired similar to results seen in young *fgl2*$^{-/-}$ mice (our unpublished data). Alteration in CD4$^+$CD25$^+$ Treg cell numbers or activity has been shown to be associated with autoimmune diseases (31). We therefore propose that loss of Treg cell function in *fgl2*$^{-/-}$ mice accounts for the increased immune reactivity and the development of the glomerulonephritis. In favor of the important role for FGL2 in Treg cell suppressive activity is the observation that Treg cells treated with Ab to FGL2 have no suppressive activity.

Increased numbers of Treg cells and Foxp3 expression in *fgl2*$^{-/-}$ mice were observed. Increased levels of IL-2 in supernatants from the MLR cultures of *fgl2*$^{-/-}$ responder cells (our unpublished data) might explain the increased numbers of Treg cells, which bear CD25 and thus proliferate in response to IL-2. However, Treg cells from *fgl2*$^{-/-}$ mice exhibited decreased suppressive activity compared with Treg cells from *fgl2*$^{+/+}$ mice. These results suggest that FGL2 is an important effector molecule of Treg cells and that the increased numbers of Treg cells and Foxp3 expression might serve as a compensatory mechanism for the diminished Treg cell activity in *fgl2*$^{-/-}$ mice. Other molecules including TGF-β, IL-10, CTLA-4, LAG-3, CD39, and galectin-1 have also been reported to account for the regulatory activity of Treg cells. However, Ab to these molecules in some cases had no effect or only minimally inhibited Treg cell activity in vitro in contrast to Ab to FGL2 (32–36). The data generated in this report and by others suggest that the suppressive activity of Treg cells is complex involving many redundant pathways. In support of this concept, Treg cells from both *TGF-β*$^{-/-}$ and *CTLA-4*$^{-/-}$ mice exhibited normal activity (36).

In addition to CD4$^+$CD25$^+$ Treg cells, *fgl2* might be important to the function and/or development of other Treg cell subsets. We have observed a marked increase in the expression levels of *fgl2* mRNA and FGL2 protein in CD4$^-$CD8$^-$ double negative T cells and a loss of *fgl2* expression in a double negative mutant clone, which is devoid of suppressor activity (our unpublished data). Recently, CD8$\alpha\alpha^+$ T cells were likewise shown to express increased levels of *fgl2* suggesting that *fgl2* may have an important role in other Treg cell populations (20). The fact that CD8$\alpha\alpha^+$ T cells are critical for intestinal tolerance suggests that *fgl2* may also play a role in maintaining tolerance in the intestine.

Clinical evidence also suggests that FGL2 negatively regulates the immune system. Hepatitis B and hepatitis C patients express increased levels of FGL2 (19, 37) and DC derived from patients with chronic HCV and HBV infections have attenuated responses to maturation stimuli (lower CD86 expression), impaired T cell stimulating capabilities, and decreased IFN-γ production (38, 39). Furthermore, these chronic viral HBV- and HCV-infected patients are incapable of mounting protective T cell responses (40). Kohno et al. (41) have demonstrated a loss of *fgl2* transcripts in patients with acute and chronic adult T cell leukemia, a lymphoproliferative disorder of Th cells, suggesting a potential role for FGL2 in the regulation of T cell proliferation.

The mechanism whereby FGL2 exerts its immunoregulatory activity was also investigated in this study. BM chimera studies demonstrated that hemopoietic cells from *fgl2*$^{-/-}$ mice mediate the increased immune reactivity seen in *fgl2*$^{-/-}$ mice. The increased numbers of Ab-producing B cells in response to TI Ags, shown by ELISPOT and our DC studies, suggest that FGL2 fulfills its immunoregulatory function through its effects on APC. In favor of this notion, FGL2 has been demonstrated to bind specifically to the low-affinity FcγRIIB and FcγRIII, which are present on DC and B cells (Figs. 7 and 8). The binding of FGL2 to these receptors led to inhibition of DC maturation and induction of B cell apoptosis. It has also been reported (42) that glomerular mesangial cells within the kidney express high levels of inhibitory FcγRIIB receptors, and Bolland and Ravetch (43) have shown that *FcγRIIB*$^{-/-}$ mice on a C57BL/6 background develop glomerulonephritis. Thus, we would expect that *fgl2*$^{-/-}$ mice, which lack the ligand for FcγRIIB, would develop glomerulonephritis similar to *FcγRIIB*$^{-/-}$ mice.

Collectively, the results of the present study suggest that *fgl2* accounts, at least in part, for the suppressive activity of Treg cells. Loss of FGL2 results in significant immune dysregulation and glomerulonephritis. These studies suggest that FGL2 exerts its immunosuppressive activity through binding to the low-affinity FcγRIIB receptor, which is known to be expressed on APC and is an important immunoregulatory receptor.

Acknowledgment

We are grateful to Charmaine Beal for preparation of this manuscript.

Disclosures

The authors have no financial conflict of interest.

References

1. Chiquet-Ehrismann, R., C. Hagios, and K. Matsumoto. 1994. The tenascin gene family. *Perspect. Dev. Neurobiol.* 2: 3–7.
2. Doolittle, R. F. 1983. The structure and evolution of vertebrate fibrinogen. *Ann. NY Acad. Sci.* 408: 13–27.
3. Koyama, T., L. R. Hall, W. G. Haser, S. Tonegawa, and H. Saito. 1987. Structure of a cytotoxic T-lymphocyte-specific gene shows a strong homology to fibrinogen β and γ-chains. *Proc. Natl. Acad. Sci. USA* 84: 1609–1613.
4. Ding, J. W., Q. Ning, M. F. Liu, A. Lai, J. Leibowitz, K. M. Peltekian, E. H. Cole, L. S. Fung, C. Holloway, P. A. Marsden, et al. 1997. Fulminant hepatic failure in murine hepatitis virus strain 3 infection: tissue-specific expression of a novel fgl2 prothrombinase 1. *J. Virol.* 71: 9223–9230.
5. Fung, L. S., G. Neil, J. L. Leibowtiz, E. H. Cole, S. Chung, A. Crow, and G. A. Levy. 1991. Monoclonal antibody analysis of a unique macrophage procoagulant activity induced by murine hepatitis virus strain 3 infection. *J. Biol. Chem.* 266: 1789–1795.
6. Ding, J. W., Q. Ning, M. F. Liu, A. Lai, K. Peltekian, L. Fung, C. Holloway, H. Yeger, M. J. Phillips, and G. A. Levy. 1998. Expression of the fgl2 and its protein product (prothrombinase) in tissues during murine hepatitis virus strain-3 (MHV-3) infection. *Adv. Exp. Med. Biol.* 440: 609–618.
7. Marsden, P. A., Q. Ning, L. S. Fung, X. Luo, Y. Chen, M. Mendicino, A. Ghanekar, J. A. Scott, T. Miller, C. W. Chan, et al. 2003. The Fgl2/fibroleukin prothrombinase contributes to immunologically mediated thrombosis in experimental and human viral hepatitis. *J. Clin. Invest.* 112: 58–66.
8. Parr, R. L., L. Fung, J. Reneker, N. Myers-Mason, J. L. Leibowitz, and G. Levy. 1995. Association of mouse fibrinogen-like protein with murine hepatitis virus-induced prothrombinase activity. *J. Virol.* 69: 5033–5038.
9. Levy, G. A., J. L. Leibowitz, and T. S. Edgington. 1981. Induction of monocyte procoagulant activity by murine hepatitis virus type 3 parallels disease susceptibility in mice. *J. Exp. Med.* 154: 1150–1163.
10. Ninq, Q., M. Liu, M. M. C. Lai, P. A. Marsden, E. Cole, J. Tseng, B. Pereira, M. Belyavskyi, J. L. Leibowitz, M. J. Phillips, and G. A. Levy. 1999. The nucleocapsid protein of murine hepatitis virus type 3 induces transcription of the novel fgl2 prothrombinase gene. *J. Biol. Chem.* 274: 9930–9936.
11. Mendicino, M., M. Liu, A. Ghanekar, W. He, C. Koscik, I. Shalev, M. Javadi, J. Turnbull, W. Chen, L. Fung, et al. 2005. Targeted deletion of Fgl-2/fibroleukin in the donor modulates immunologic response and acute vascular rejection in cardiac xenografts. *Circulation* 112: 248–256.
12. Ghanekar, A., M. Mendicino, H. Liu, W. He, M. Liu, R. Zhong, M. J. Phillips, G. A. Levy, and D. R. Grant. 2004. Endothelial induction of fgl2 contributes to thrombosis during acute vascular xenograft rejection. *J. Immunol.* 172: 5693–5701.
13. Ning, Q., Y. Sun, M. Han, L. Zhang, C. Zhu, W. Zhang, H. Guo, J. Li, W. Yan, F. Gong, et al. 2005. Role of fibrinogen-like protein 2 prothrombinase/fibroleukin in experimental and human allograft rejection. *J. Immunol.* 174: 7403–7411.
14. Clark, D. A., K. Foerster, L. Fung, W. He, L. Lee, M. Mendicino, U. R. Markert, R. M. Gorczynski, P. A. Marsden, and G. A. Levy. 2004. The fgl2 prothrombinase/fibroleukin gene is required for lipopolysaccharide-triggered abortions and for normal mouse reproduction. *Mol. Hum. Reprod.* 10: 99–108.
15. Knackstedt, M. K., A. C. Zenclussen, K. Hertwig, E. Hagen, J. W. Dudenhausen, D. A. Clark, and P. C. Arck. 2003. Th1 cytokines and the prothrombinase fgl2 in

stress-triggered and inflammatory abortion. *Am. J. Reprod. Immunol.* 49: 210–220.
16. Hancock, W. W., F. M. Szaba, K. N. Berggren, M. A. Parent, I. K. Mullarky, J. Pearl, A. M. Cooper, K. H. Ely, D. L. Woodland, I. J. Kim, et al. 2004. Intact type 1 immunity and immune-associated coagulative responses in mice lacking IFN γ-inducible fibrinogen-like protein 2. *Proc. Natl. Acad. Sci. USA* 101: 3005–3010.
17. Marazzi, S., S. Blum, R. Hartmann, D. Gundersen, M. Schreyer, S. Argraves, V. von Fliedner, R. Pytela, and C. Ruegg. 1998. Characterization of human fibroleukin, a fibrinogen-like protein secreted by T lymphocytes. *J. Immunol.* 161: 138–147.
18. Ruegg, C., and R. Pytela. 1995. Sequence of a human transcript expressed in T-lymphocytes and encoding a fibrinogen-like protein. *Gene* 160: 257–262.
19. Chan, C. W., L. S. Kay, R. G. Khadaroo, M. W. Chan, S. Lakatoo, K. J. Young, L. Zhang, R. M. Gorczynski, M. Cattral, O. Rotstein, and G. A. Levy. 2003. Soluble fibrinogen-like protein 2/fibroleukin exhibits immunosuppressive properties: suppressing T cell proliferation and inhibiting maturation of bone marrow-derived dendritic cells. *J. Immunol.* 170: 4036–4044.
20. Denning, T. L., S. W. Granger, D. Mucida, R. Graddy, G. Leclercq, W. Zhang, K. Honey, J. P. Rasmussen, H. Cheroutre, A. Y. Rudensky, and M. Kronenberg. 2007. Mouse TCRαβ$^+$CD8αα intraepithelial lymphocytes express genes that down-regulate their antigen reactivity and suppress immune responses. *J. Immunol.* 178: 4230–4239.
21. Herman, A. E., G. J. Freeman, D. Mathis, and C. Benoist. 2004. CD4$^+$CD25$^+$ T regulatory cells dependent on ICOS promote regulation of effector cells in the prediabetic lesion. *J. Exp. Med.* 199: 1479–1489.
22. Fontenot, J. D., J. P. Rasmussen, M. A. Gavin, and A. Y. Rudensky. 2005. A function for interleukin 2 in Foxp3-expressing regulatory T cells. *Nat. Immunol.* 6: 1142–1151.
23. Fontenot, J. D., J. P. Rasmussen, L. M. Williams, J. L. Dooley, A. G. Farr, and A. Y. Rudensky. 2005. Regulatory T cell lineage specification by the forkhead transcription factor foxp3. *Immunity* 22: 329–341.
24. Gavin, M. A., J. P. Rasmussen, J. D. Fontenot, V. Vasta, V. C. Manganiello, J. A. Beavo, and A. Y. Rudensky. 2007. Foxp3-dependent programme of regulatory T-cell differentiation. *Nature* 445: 771–775.
25. Williams, L. M., and A. Y. Rudensky. 2007. Maintenance of the Foxp3-dependent developmental program in mature regulatory T cells requires continued expression of Foxp3. *Nat. Immunol.* 3: 277–284.
26. Zheng, Y., S. Z. Josefowicz, A. Kas, T. T. Chu, M. A. Gavin, and A. Y. Rudensky. 2007. Genome-wide analysis of Foxp3 target genes in developing and mature regulatory T cells. *Nature* 445: 936–940.
27. Cole, E. H., M. F. Glynn, C. A. Laskin, J. Sweet, N. Mason, and G. A. Levy. 1990. Ancrod improves survival in murine systemic lupus erythematosus. *Kidney Int.* 37: 29–35.
28. Butcher, E. C., R. V. Rouse, R. L. Coffman, C. N. Nottenburg, R. R. Hardy, and I. L. Weissman. 2005. Surface phenotype of Peyer's patch germinal center cells: implications for the role of germinal centers in B cell differentiation. 1982. *J. Immunol.* 175: 1363–1372.
29. Liu, H., L. Zhang, M. Cybulsky, R. Gorczynski, J. Crookshank, J. Manuel, D. Grant, and G. Levy. 2006. Identification of the receptor for FGL2 and implications for susceptibility to mouse hepatitis virus (MHV-3)-induced fulminant hepatitis. *Adv. Exp. Med. Biol.* 581: 421–425.
30. Procopio, W. N., P. I. Pelavin, W. M. Lee, and N. M. Yeilding. 1999. Angiopoietin-1 and -2 coiled coil domains mediate distinct homo-oligomerization patterns, but fibrinogen-like domains mediate ligand activity. *J. Biol. Chem.* 274: 30196–30201.
31. Sakaguchi, S. 2005. Naturally arising Foxp3-expressing CD25$^+$CD4$^+$ regulatory T cells in immunological tolerance to self and nonself. *Nat. Immunol.* 6: 345–352.
32. Huang, C. T., C. J. Workman, D. Flies, X. Pan, A. L. Marson, G. Zhou, E. L. Hipkiss, S. Ravi, J. Kowalski, H. I. Levitsky, et al. 2004. Role of LAG-3 in regulatory T cells. *Immunity* 21: 503–513.
33. Tang, Q., E. K. Boden, K. J. Henriksen, H. Bour-Jordan, M. Bi, and J. A. Bluestone. 2004. Distinct roles of CTLA-4 and TGF-β in CD4$^+$CD25$^+$ regulatory T cell function. *Eur. J. Immunol.* 34: 2996–3005.
34. Deaglio, S., K. M. Dwyer, W. Gao, D. Friedman, A. Usheva, A. Erat, J. F. Chen, K. Enjyoji, J. Linden, M. Oukka, et al. 2007. Adenosine generation catalyzed by CD39 and CD73 expressed on regulatory T cells mediates immune suppression. *J. Exp. Med.* 204: 1257–1265.
35. Garin, M. I., C. C. Chu, D. Golshayan, E. Cernuda-Morollon, R. Wait, and R. I. Lechler. 2007. Galectin-1: a key effector of regulation mediated by CD4$^+$CD25$^+$ T cells. *Blood* 109: 2058–2065.
36. Miyara, M., and S. Sakaguchi. 2007. Natural regulatory T cells: mechanisms of suppression. *Trends Mol. Med.* 13: 108–116.
37. Levy, G. A., M. Liu, J. Ding, S. Yuwaraj, J. Leibowitz, P. A. Marsden, Q. Ning, A. Kovalinka, and M. J. Phillips. 2000. Molecular and functional analysis of the human prothrombinase gene (HFGL2) and its role in viral hepatitis. *Am. J. Pathol.* 156: 1217–1225.
38. Auffermann-Gretzinger, S., E. B. Keeffe, and S. Levy. 2001. Impaired dendritic cell maturation in patients with chronic, but not resolved, hepatitis C virus infection. *Blood* 97: 3171–3176.
39. Kakumu, S., S. Ito, T. Ishikawa, Y. Mita, T. Tagaya, Y. Fukuzawa, and K. Yoshioka. 2000. Decreased function of peripheral blood dendritic cells in patients with hepatocellular carcinoma with hepatitis B and C virus infection. *J. Gastroenterol. Hepatol.* 15: 431–436.
40. Sugimoto, K., D. E. Kaplan, F. Ikeda, J. Ding, J. Schwartz, F. A. Nunes, H. J. Alter, and K. M. Chang. 2005. Strain-specific T-cell suppression and protective immunity in patients with chronic hepatitis C virus infection. *J. Virol.* 79: 6976–6983.
41. Kohno, T., R. Moriuchi, S. Katamine, Y. Yamada, M. Tomonaga, and T. Matsuyama. 2000. Identification of genes associated with the progression of adult T cell leukemia (ATL). *Jpn. J. Cancer Res.* 91: 1103–1110.
42. Radeke, H. H., I. Janssen-Graalfs, E. N. Sowa, N. Chouchakova, J. Skokowa, F. Loscher, R. E. Schmidt, P. Heeringa, and J. E. Gessner. 2002. Opposite regulation of type II and III receptors for immunoglobulin G in mouse glomerular mesangial cells and in the induction of anti-glomerular basement membrane (GBM) nephritis. *J. Biol. Chem.* 277: 27535–27544.
43. Bolland, S., and J. V. Ravetch. 2000. Spontaneous autoimmune disease in Fc(γ)RIIB-deficient mice results from strain-specific epistasis. *Immunity* 13: 277–285.